Novel Retinal and Cone Photoreceptor Transcripts Revealed by Human Macular Expression Profiling

Daniel M. Hornan,[1] *Stuart N. Peirson,*[2] *Alison J. Hardcastle,*[1] *Robert S. Molday,*[3] *Michael E. Cheetham,*[1] *and Andrew R. Webster*[1]

Purpose. The macula is essential for visual acuity. It contains many more cone photoreceptors than does the peripheral retina. In this study, macular gene expression was compared with that in the rod-rich peripheral retina.

Methods. Two-millimeter foveomacular and four-millimeter macular punches from human donor eyes, in addition to sections of midperipheral retina, were used to study differential gene expression. Multiple microarray experiments were combined with quantitative PCR and bioinformatic analyses. In the present study, the expression of both known and previously unidentified retinal genes was determined.

Results. Several macula enriched transcripts were revealed. Nuclear pore complex interacting protein (NPIP) and eukaryotic translation initiation factor 2α kinase (GCN2) were expressed at levels approaching that of red/green cone opsin in the macula. The protein products of several genes highlighted using these expression analyses were also localized in the retina. Both NPIP and histone deacetylase 9 (HDAC9) proteins were detected in cone photoreceptor outer segments.

Conclusions. Characterizing macula enriched transcripts is an important stepping-stone in understanding the molecular basis for visual acuity in the retina. The approach also provides excellent candidates for diseases that affect the macula and fovea such as age-related macular degeneration (AMD). Indeed, several of these transcripts, such as NPIP and GCN2, have genomic loci that are consistent with being candidate genes for AMD. (*Invest Ophthalmol Vis Sci.* 2007;48:5388–5396) DOI: 10.1167/iovs.07-0355

The human macula is the specialized cone-rich region of the central retina (4 mm) that is used for reading, writing, and face recognition. It supports visual acuity due in part to the high density of cones in the foveal region.[1]

Although many expressed sequence tags (ESTs) have been identified from central retinal cDNA libraries (www.ncbi.nlm.nih.gov/dbEST/ National Center for Biotechnology Information [NCBI], Bethesda, MD), most are unlikely to vary significantly in their expression throughout the retina. Despite this, Northern blot analysis has shown that there are significant differences in gene expression between the central and peripheral retina.[2] More recently, serial analysis of gene expression (SAGE) comparing the perimacular region (6 mm) with the peripheral retina has revealed several genes that are overrepresented in the central retina (www.ncbi.nlm.nih.gov/geo/ NCBI), HMAC2_SAGE).[3] However, a greater number of gene tags have been found to be differentially expressed between two separate peripheral retinas (HPR1/2_SAGE).

Age-related macular degeneration (AMD) is a multifactorial disease that causes loss of central vision. It is the most common cause of blindness in the developed world and is responsible for more than 50% of blind or partial sight registrations in the UK.[4] Approximately 10% of people older than 65 and 30% older than 75 show retinal changes consistent with AMD. Moreover, the prevalence of AMD is increasing.[5] Twin and sibling studies suggest that the genetic component of AMD is at least one quarter,[6–9] with smoking being the only well established environmental risk factor. Several whole genome scans for linkage in families with AMD have defined four main chromosomal regions of susceptibility to AMD: 1q13, 6p, 10q26, and 16p12. Recently, complement factor H (CFH/HF1) has been implicated as the susceptibility gene at 1q13, and some genetic variants are likely to double the risk of having AMD.[10–13] Variants in two other regulatory components of the alternative complement pathway BF and C2 have also been associated with increased or decreased risk of AMD.[14] At the 10q26 locus HTRA1, a serine protease activated by cellular stress has been associated with major susceptibility to AMD independent of CFH.[15,16]

As AMD susceptibility is due to both environmental and hereditary factors, gene expression analyses may help to understand the molecular context of the disease. Microarray-initiated experiments have been used in the retina to identify both disease-causing (autosomal dominant retinitis pigmentosa[17]) and major regulatory (homeobox *CRX*[18,19]) genes.

In the present study, we identified retinal genes that are consistently overexpressed in the macula, some of which are also abundant transcripts. An important observation was that two of the protein products of these transcripts are enriched in cone photoreceptor outer segments. One of these genes, nuclear pore complex interacting protein (NPIP), lies at an as yet undefined susceptibility locus for AMD (16p12).

Methods

Tissue Preparation

Normal human donor eyes were obtained from the Eye Bank of British Columbia in accordance with the Declaration of Helsinki and local medical ethics boards. Globes were immersed in preservative (RNA_{later}; Ambion, Huntingdon, UK) and placed in the refrigerator after enucleation. The eyes were dissected on ice and a full-thickness punch of the posterior globe was made with an 8-mm skin biopsy punch. The neural retina was then floated off the retinal pigment epithelium with the aid of the vitreous humor. A further 4- or 2-mm punch was taken from the neural retina centered at the macula lutea. Sections of midperipheral

From the [1]Institute of Ophthalmology, Molecular Genetics, University College, London, United Kingdom; the [2]Department of Visual Neuroscience, Imperial College, London, United Kingdom; and the [3]Macular Research Centre, University of British Columbia, Vancouver, British Columbia, Canada.

Supported by grants from Research into Ageing (Help the Aged, UK) and E. A. Baker/CIHR (Canadian Institutes of Health Research).

Submitted for publication March 24, 2007; revised July 5, 2007; accepted October 8, 2007.

Disclosure: **D.M. Hornan**, None; **S.N. Peirson** , None; **A.J. Hardcastle**, None; **R.S. Molday**, None; **M.E. Cheetham**, None; **A.R. Webster**, None

The publication costs of this article were defrayed in part by page charge payment. This article must therefore be marked "*advertisement*" in accordance with 18 U.S.C. §1734 solely to indicate this fact.

Corresponding author: Daniel M. Hornan, Molecular Genetics, Institute of Ophthalmology, 11-43 Bath St., London EC1V 9EL, UK; d.hornan@doctors.org.uk.

Investigative Ophthalmology & Visual Science, December 2007, Vol. 48, No. 12

retina were removed with forceps from cut quarters of the globe. RNA was extracted using a PCR kit (RNAqueous-4PCR; Ambion) according to the manufacturer's protocol, including the DNase treatment step. RNA was quantified, and the quality assessed by spectrophotometry and formaldehyde agarose gel electrophoresis.

Northern Blot Analysis

Probes were designed from human rod and long/medium-wave cone opsin of lengths 345 and 424 bp respectively (primers available on request). These probes were amplified individually by RT-PCR from retinal RNA (SuperScript; Invitrogen). The probes were labeled with α32-P-dCTP using a labeling kit (Prime-a-Gene; Promega, Madison, WI) and cleaned up with a nucleotide removal kit (QIAquick; Qiagen, Crawley, CA). For each probe 5 μg of total RNA, from peripheral retina and 4 mm macula, were electrophoresed in adjacent lanes of a formaldehyde agarose gel and transferred to a nylon membrane. The probes were hybridized (ULTRAhyb; Ambion) according to the manufacturer's protocol.

Microarrays

Microarray slides were designed at the Gene Array Facility, University of British Columbia (Vancouver, BC, Canada). The set consisted of 13,899 70-mers from a probe set (Operon ver. 1.1; Qiagen), and these were spotted robotically in duplicate onto glass slides, together with control probes contained in the set. Each slide was subject to strict quality control. Targets were prepared with 7.5 μg total RNA, with either Cy3 or Cy5 dUTP and reverse transcriptase (Superscript II; Invitrogen) and were cleaned up with a PCR purification kit (QiaQuick; Qiagen) in light-shielded conditions and precipitated overnight with ethanol and sodium acetate. Each target was resuspended in 50 μL hybridization solution containing: 25 μL formamide, 12.5 μL 20× SSC, 0.5 μL 10% SDS, 5 μL of 2 g/L BSA, 5 μL of 5 g/L yeast tRNA and 2 μL of 10 g/L salmon testes DNA. The slides were denatured at 95°C just before use. The Cy3 and Cy5 target were mixed together and hybridized to the slide under a coverslip in a moisture-rich environment overnight at 42°C. The coverslip was removed by floating the slide in 0.2× SSC. The slide was then washed three times for 5 minutes with 0.1× SSC and 0.1% SDS and three times for 5 minutes in 0.1× SSC. The slide was centrifuged in a tube at 2000 rpm for 5 minutes to dry before imaging (ChipReader; Virtek Vision Corp, Waterloo, ON, Canada).

Grids were overlaid onto images of each slide by computer (ImageGene software; BioDiscovery, Los Angeles, CA), which was also used to quantify each spot in the two channels corresponding to the Cy3 and Cy5 fluorescence images. The individual spot intensities were subjected to an in-house background correction algorithm that uses the lowest 10% of intensity values for each subgrid as background. In microarray analysis, typically less than half of the probes light up with a particular target. The data were parsed by using custom-written algorithms to associate each spot with its corresponding probe identity. Data were then calibrated by using several different statistical methods, including log-ratios and variance stabilization (www.dkfz-heidelberg.de/mga/whuber/ German Cancer Research Center, Heidelberg, Germany).[20] Data were analyzed by writing scripts in the R statistical computing language (www.r-project.org). The processed data from each slide were inserted into an SQL database to facilitate data mining.

Quantitative PCR

First, intron-spanning primers (Supplementary Data, online at http://www.iovs.org/cgi/content/full/48/12/5388/DC1) were designed within two adjacent exons of rhodopsin. Two micrograms of pooled peripheral retinal and pooled foveomacular RNA (as measured by spectrophotometry) was reverse transcribed with random decamers (RetroScript; Ambion). Peripheral retinal cDNA was amplified with the intron-spanning rhodopsin primer pair to check for genomic DNA contamination.

Primer pairs (Supplementary Data) were generated to regions of the cDNAs chosen for qPCR analysis, including four internal controls (18S rRNA, acidic ribosomal phosphoprotein, β-actin, and ubiquitin C), by using the GCG-Wisconsin package (Accelrys, Campbell, CA). Peripheral retinal cDNA was used to find optimal primer pairs to amplify each chosen cDNA specifically, with SYBR-green PCR master mix (Applied Biosystems, Inc.; Foster City, CA). Products were checked on agarose. Optimized reactions were melted (model 7700; ABI) to check for a single product and to discern its melting temperature. To double check the specificity of the primers, four PCR products (RHO, OPN1LW, 6q, and BHM2) were subjected to direct sequencing.

Quantitative PCR reactions were performed in triplicate for each gene with peripheral, foveomacular, and no-template control samples (model 7700; ABI). An additional PCR step was inserted at the appropriate melting temperature at which to measure the fluorescence of the product. Cyclical fluorescence values were recorded and preprocessed with the system software (ABI). These data were then analyzed on a custom-written spreadsheet (Excel; Microsoft, Redmond, WA; DART-PCR[21]) to extrapolate the initial fluorescence values and normalize them to the internal controls.

Immunocytochemistry

A rabbit polyclonal antibody to the C terminus of HDAC9 (NP_848512, 1069 amino acids) was obtained from the laboratory of Arthur Zelent (Institute of Cancer Research). It was raised to the peptide DVEQPFAQEDSRTAG, from amino acid 1046-1060 that detects the full-length protein.[22] For NPIP, a 15-amino-acid synthetic peptide, CSLPFHPQRMIISRN, corresponding to the C terminus was used for production of rabbit polyclonal antisera (Sigma-Aldrich, St. Louis, MO).

For immunocytochemistry, tissue culture cells were washed, fixed, and permeabilized using 3.7% paraformaldehyde and 0.1% Triton X-100 in eight-well chamber glass slides (Nunc, Naperville, IL) before blocking with normal donkey serum (NDS 1:10) in BSA 3%, to counter nonspecific binding of the primary antibody. All incubation steps were performed at room temperature, and appropriate washing steps were included. 4′,6-Diamidino-2-phenylindole (DAPI) was used to counterstain nuclei. The retinal cryosections were processed under similar conditions except that Triton was not used. Control experiments were performed in parallel with omission of the primary antibody only. A confocal laser scanning microscope (LSM510; Carl Zeiss Meditec) was used to image the slides.

Cloning

Primers were designed (Supplementary Data) to add restriction sites to each end of NPIP to facilitate subcloning into the GFP fusion expression vector (pEGFP-C2; BD-Clontech, Palo Alto, CA) that fuses the insert to the C terminus of GFP. A 5′ *Eco*RI site and 3′ *Sal*I site were chosen, as they are compatible with in-frame subcloning. NPIP was amplified from brain cDNA, and the products were gel purified and cloned into a vector (pGEM-T Easy; Promega). DNA extracted from the amplified vector was sequenced bidirectionally before proceeding to the subcloning step.

Results

Confirmation of Known Differential Gene Expression in the Macula

No signs of retinal disease were observed in the donor eyes procured. The age varied from 40 to 77 years (mean, 64) and the sex distribution was approximately even. The time between death and preservation (RNA_{later}; Ambion), ranged from 4 to 12 hours (mean 7.5). Tens of micrograms of high quality RNA were obtained from each of 10 peripheral retinas (Supplementary Data), from two pooled 4-mm macular punches, and from 12 pooled 2-mm foveomacular punches. No DNA was evident by agarose gel electrophoresis and RT-PCR with intron-

TABLE 1. Duplicate Microarray Experiments

	Cy3	Cy5
1	Peripheral retina 1	Peripheral retina 1
2	Peripheral retina 1	Peripheral retina 2
3	4 mm Pooled macula	Peripheral retina 1
4	4 mm Pooled macula	Peripheral retina 2
5	2 mm Pooled foveomacula	Peripheral retina 1
6	2 mm Pooled foveomacula	Peripheral retina 2

Peripheral retina 1 was from a 72-year-old woman who died of respiratory arrest secondary to lung cancer and whose eyes were enucleated and immersed in preservative within 7 hours of death. Peripheral retina 2 was from a 57-year-old man who died of a stroke secondary to carotid artery stenosis and whose eyes were enucleated and immersed in preservative within 6 hours of death. For agarose gels of the RNA (Supplementary Data, online at http://www.iovs.org/cgi/content/full/48/12/5388/DC1).

spanning rhodopsin primers yielded only an exonic fragment (Supplementary Data). Northern blot analysis of pooled 4-mm macular and peripheral retinal RNA showed enhanced red/green cone opsin signal in the macula and, conversely, increased rhodopsin signal in the peripheral retina (Supplementary Data).

Genes Enriched in Macula and Fovea

Six duplicate microarray experiments were performed to find differentially expressed genes in the human macula (Table 1). Expression data (Fig. 1) were plotted as the difference in expression between channels: $M = b(\text{Cy5}) - b(\text{Cy3})$ against the rank of the mean expression

$$A = \frac{b(\text{Cy3}) + b(\text{Cy5})}{2}$$

where $b(x)$ was either a logarithmic $b(x) = \log_2(x)$ or variance stabilization $b(x) = \sinh^{-1}(a + bx)$ (Ref. 20) normalization function. This standard method of plotting microarray data uses ranks rather than the absolute values of mean expression, as it makes it easier to visualize differential expression (by reducing the central bulge in the data due to most genes being of midlevel expression).

The log transformations (Fig. 1) highlighted many low-expression genes with large differences in expression, resulting in typical funnel-shaped plots.[23] The variance-stabilized data resulted in much flatter graphs, especially for the control experiments (1 and 2). A characteristic central bulge of differentially expressed genes at midlevel expression appeared in the central versus peripheral experiments. There were also several highly expressed genes differentially expressed, especially in experiments 4 to 6.

Data were mined by querying an SQL database for probes that showed consistent differential expression (Table 2), according to strict selection criteria based on diagnostic plots and analyses. First, genes that did not exhibit an absolute fluorescence of at least 200 above background in at least two channels were discarded, because this was less than twice the highest background value. Second, genes that showed variability of one expression unit (twofold) or greater were excluded. All central retina enriched genes included had expression ratios of >3 (eightfold increase) and also had higher expression ratios in the foveomacula-versus-periphery compared with the macula-versus-periphery experiments. Peripheral enriched genes

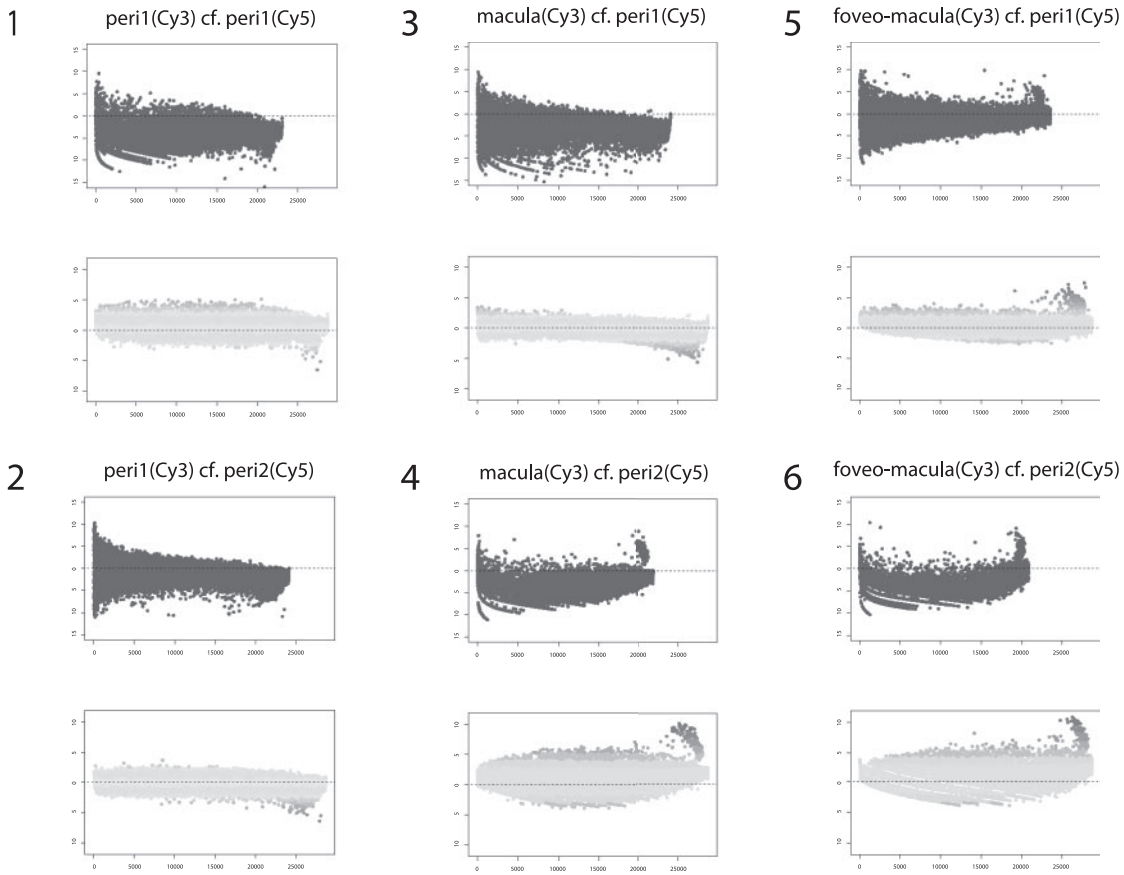

FIGURE 1. Relative versus rank mean expression ratios in six microarray experiments. *Top*: log ratios; *bottom*: variance-stabilized ratios.

TABLE 2. Summary of Microarray and Data, Including Opsin Controls and Candidate Differentially Expressed Genes

Name	Symbol	Accession	Exp	Cy3	Cy5	Vsn3	Vsn5	Vsn3/Vsn5
Rhodopsin	*RHO*	NM_000539	1,2	396	5968	4.34	3.78	−0.54 ± 0.60
			3,4	53	594	2.82	2.85	−0.04 ± 0.60
			5,6	213	1758	3.08	4.01	−0.92 ± 0.60
Long-wave cone opsin	*OPNILW*	MI3305	1,2	47	253	1.54	1.37	−0.12 ± 0.89
			3,4	26	320	1.47	1.26	0.21 ± 0.89
			5,6	177	142	2.69	1.48	1.21 ± 0.89
Yes-associated 65	*YAP65*	X80507	1,2	32	189	1.01	1.06	−0.36 ± 0.5
			3,4	349	968	4.60	3.30	1.31 ± 0.5
			5,6	745	327	5.33	1.81	3.52 ± 0.5
Histone deacetylase 9	*HDAC9*	AC004744	1,2	90	595	2.66	2.01	−0.07 ± 0.65
			3,4	288	915	4.46	1.75	2.70 ± 0.65
			5,6	681	199	5.27	1.90	3.37 ± 0.65
SLT-ROBO GTPase	*SRGAP2*	AB032982	1,2	672	2222	4.03	3.87	0.88 ± 0.88
			3,4	1750	6301	6.10	4.49	1.60 ± 0.88
			5,6	1234	496	5.64	2.46	3.18 ± 0.88
Hypothetical protein	*FLJ20103*	AK000110	1,2	750	3192	4.29	4.12	0.48 ± 0.48
			3,4	705	4257	5.29	4.08	1.20 ± 0.48
			5,6	1238	418	5.79	2.61	3.18 ± 0.48
Nuc. pore complex	*NPIP*	NM_006985	1,2	484	1868	3.67	3.6	0.28 ± 0.28
			3,4	750	3161	5.32	4.24	1.08 ± 0.28
			5,6	2264	879	6.20	3.08	3.12 ± 0.28
cDNA from 6q22.1	*6q22*	AL133101	1,2	896	2939	4.51	4.04	0.62 ± 0.62
			3,4	1121	5100	5.70	4.33	1.37 ± 0.62
			5,6	1212	494	5.82	2.73	3.09 ± 0.62
β-HomoCys CH3-t'ase	*BHMT2*	AK000008	1,2	3485	16485	5.9	5.67	0.59 ± 0.59
			3,4	6946	27782	7.57	6.15	1.42 ± 0.59
			5,6	13332	4995	8.22	5.16	3.06 ± 0.59
GCN2 eiF2α kinase	*GCN2*	AB037759	1,2	1670	6990	5.03	4.91	0.71 ± 0.71
			3,4	2306	9914	6.45	5.08	1.37 ± 0.71
			5,6	4277	1636	6.95	3.92	3.03 ± 0.71
Carboxylesterase	*CRP*	NM_016280	1,2	1221	5159	4.7	4.57	0.79 ± 0.79
			3,4	2342	10425	6.47	5.10	1.37 ± 0.79
			5,6	3432	1310	6.88	3.87	3.01 ± 0.79
Retinitis pigmentosa 2	*RP2*	AJ007590	1,2	2015	9052	5.27	5.15	0.32 ± 0.32
			3,4	3318	13635	6.86	5.60	1.26 ± 0.32
			5,6	6912	2554	7.62	4.62	3.01 ± 0.32
S-antigen (rod-arrestin)	*SAG*	X12453	1,2	1107	7351	4.98	4.64	−0.09 ± 0.34
			3,4	36	282	2.41	2.09	0.32 ± 0.34
			5,6	57	537	0.81	2.80	−2.00 ± 0.34

Experiments 1 and 2 are controls, 3 and 4 are macular (4-mm) *versus* peripheral and 5 and 6 are foveomacular (2-mm) *versus* peripheral retina. *Cy3* and *Cy5* are the mean signal values, for each background-corrected channel, from the two grouped duplicate experiments. The Vsn3 and Vsn5 columns are the variance-stabilized expression values for each channel. Vsn3:Vsn5 is the variance stabilized expression ratio; a positive value enumerates over-expression in the Cy3-labeled sample. The Cy3 channel represents the macula or foveomacula compared with peripheral retina in the noncontrol experiments.

were included, for comparison, with an expression of −2 (fourfold decrease) or less. These strict selection criteria yielded several candidate differentially expressed genes for further analysis. Many more genes were found to be differentially expressed in macula compared with peripheral retina across the whole data set (Supplementary Data).

Highly Expressed Macular Genes

Real-time quantitative PCR (qPCR) was performed to validate the microarray data and to quantify expression relative to opsin. Optimized primers that produced sequence verified 150- to 250-bp amplicons, were chosen from larger cDNA sequences encompassing the 70-mer microarray probes. RNA from nine peripheral retinas was pooled and reverse transcribed in parallel with RNA pooled from 12 foveomacular punches. Expression levels of candidate differentially expressed genes from the microarray data, opsins, and four controls (18S rRNA, acidic ribosomal protein, β-actin and ubiquitin C) were compared in triplicate.

The data were analyzed using the DART-PCR system.[21] DART-PCR uses an amplification plot method that is more conservative in calculating the expression change (in *x*-fold) than the common $2^{-\Delta\Delta Ct}$ estimate of reaction efficiency. The expression level of each gene and the ratio in foveomacula: peripheral retina was calculated (Table 3) and plotted on a log base 2 scale (Fig. 2), where +1 is a twofold increase and −1 is a twofold decrease in expression. The fluorescence due to SYBR green is also proportional to the length of DNA fragment. By correcting for amplicon length, the percentage expression of selected genes relative to either rod or cone opsin were also calculated (Table 3). Reaction efficiency, as measured by the amplification plot method, typically varied by up to 10% between any two given probes, so that the values of relative expression are estimates.

Eight of the 10 macula enriched genes from the microarray data were found to be enriched in the foveomacula by quantitative PCR. Four genes were twofold or more overexpressed in foveomacula based on qPCR analysis. For these transcripts, the expression level as a percentage of cone opsin expression was calculated. Both *NPIP* and eukaryotic translation initiation factor 2α kinase (*GCN2*) showed high expression levels, which approached that of red/green cone opsin in the foveomacula. GCN2 phosphorylates the α subunit of eukaryotic translation initiation factor 2 and is

TABLE 3. Summary of qPCR Data

Symbol	Peri (P)	Fovea (F)	F/P	$\log_2$ (F/P)	% Opsin
OPN1LW	8.12E−01	2.72E+00	3.35	1.75	100
HDAC9	1.37E−03	4.30E−03	3.15	1.65	<1
NPIP	9.01E−01	1.97E+00	2.19	1.13	76
SRGAP3	5.37E−01	1.15E+00	2.14	1.10	34
SRGAP2	1.18E−02	2.31E−02	1.95	0.96	1
FLJ	3.19E−01	5.76E−01	1.81	0.85	—
6q22	1.80E−03	2.65E−03	1.47	0.56	—
CRP	2.67E−04	3.63E−04	1.36	0.44	—
BHM2	8.39E−05	1.14E−04	1.35	0.44	—
RP2	3.16E−03	2.36E−03	0.75	−0.42	—
YAP	3.80E−03	2.49E−03	0.65	−0.61	—
RHO	1.90E+00	4.16E−01	0.22	−2.20	100
SAG	5.70E−01	1.06E−01	0.19	−2.43	34

The first two columns show initial fluorescence $f(0)$ for peripheral and central retina, normalized to the four internal control genes (*18S, ARP, ACTB, UBC*), which is proportional to mRNA copy numbers. The third column is the ratio of $f(0)$, the expression ratio, in central/peripheral retina. The fourth column is the base-2 logarithm of this ratio. The final column is the expression level as a percentage of the appropriate opsin expression.

thought to be involved in the cellular response to stress.[24] *HDAC9* was more than threefold enriched and *SRGAP3* was approximately twofold enriched in foveomacula. *SRGAP3* is thought to play an important role in neuronal migration and axonal connectivity.[25] S-antigen (rod arrestin), the only peripheral retina enriched gene that fitted the strict microarray selection criteria, was over five times enhanced in the periphery according to the qPCR data, with expression approaching that of rhodopsin.

HDAC9 in Macula and Photoreceptors

HDACs are chromatin-remodeling factors that act as transcriptional repressors in response to signals such as cellular stress. HDAC9 was originally identified while investigating cDNAs that encode large proteins expressed in the human brain.[26] HDAC9's huge genomic size (7p21.1, 500 kb) and the degree to which it is regulated are unprecedented. This finding may indicate a wider role for HDAC9 than just histone modification.[22]

HDAC9 mRNA was eightfold enriched in the foveomacula according to the microarray data and was the most highly enriched gene after cone opsin according to the qPCR data. Full-length HDAC9 was localized to the nucleus of human neuroblastoma (SK-N-SH) cells (Fig. 3) using immunofluorescence with an antibody to the C terminus of HDAC9. Full-length HDAC9 has been localized to the nucleus by transiently transfecting simian fibroblast (COS-7) cells with an HDAC9-FLAG construct, followed by immunofluorescence with an anti-FLAG antibody.[22] Of interest, HDAC9 was also detected in association with filamentous structures in the SK-N-SH cells (Fig. 3).

We localized HDAC9 in the retina using the same antibody on human macular cryosections (Fig. 3). HDAC9 was present in many cell nuclei in the outer and inner nuclear layers, and in several nuclei of the ganglion cell layer, as determined by nuclear counterstain with DAPI. There was also some expression in the inner limiting membrane but very little HDAC9 in the plexiform layers. The highest HDAC9 expression was seen

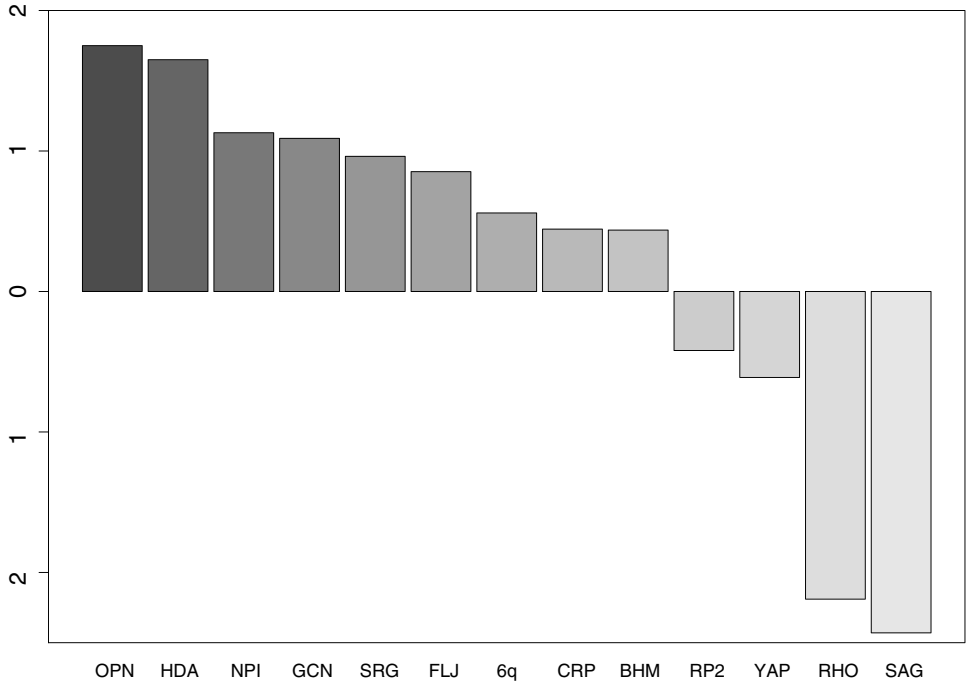

FIGURE 2. Quantitative PCR data comparing gene expression in pooled foveomacular with pooled peripheral retinal RNA. Log base 2 expression ratios are shown. OPN, OPN1; HDA, HDAC9; NPI, NPIP; GCN, GCN2; SRG, SRGAP2.

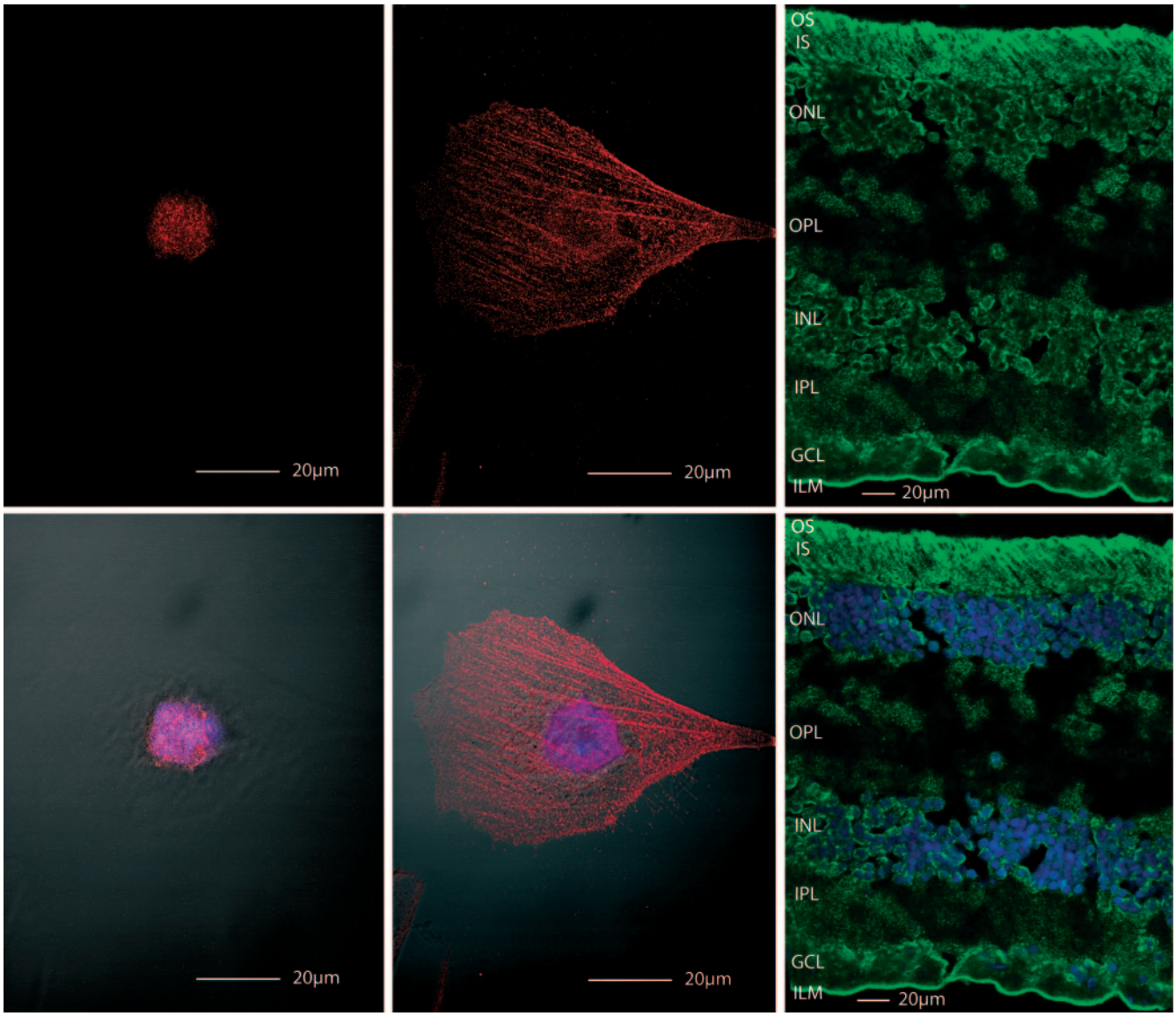

FIGURE 3. Confocal microscope images of cultured human neuroblastoma (SK-N-SH) cells (*first two columns*) and human macula (*last column*). Both cultured cells and retinal cryosections were immunostained with 1:250 rabbit anti-hdac9 serum and a fluorescent secondary antibody. The first two columns show (*red*) anti-HDAC9 staining in both the nucleus and filamentous structures in different planes of the same cell. *Right column:* anti-HDAC9 (*green*) staining in human macula, especially in photoreceptor outer segments. The merged images (*second row*) show DIC and DAPI nuclear counterstain, as well as anti-HDAC9 fluorescence.

in the photoreceptor layer and was strongest in the outer segments.

NPIP in Cone Outer Segments

NPIP is a member of a primate-specific gene family that has undergone recent adaptive evolution.[27] The protein contains one predicted transmembrane domain and is located on the nuclear envelope in cultured cells.

NPIP was eightfold overexpressed in the foveomacula compared with the peripheral retina according to the microarray data. It was the second most highly enriched gene after cone opsin according to the qPCR data. NPIP was very highly expressed in foveomacula at approximately 76% of the level of cone opsin. Endogenous NPIP was localized to the nuclear envelope region of adherent SK-N-SH cells (Supplementary Data), by using immunofluorescence with an antibody raised to the C terminus, as determined by nuclear counterstain. These data for the endogenous protein were in accordance with a previous report that localized NPIP-GFP to this subcellular location by transiently transfecting COS-7 cells.[27]

We localized NPIP in the retina with the anti-NPIP antibody on cryosections of human fovea (Fig. 4). This revealed specific staining on the sheaths of the cone outer segments. There was apparent colocalization with peanut agglutinin (PNA), which stains cone photoreceptor sheaths.

Membrane Localization Signal of Novel NPIP Isoforms in N Terminus

We cloned two novel isoforms of NPIP from cDNA. One clone (NPIP1, Supplementary Data) is very similar to the reference sequence AF132984, except that there are an extra 47 bases within exon 8. This is predicted to encode a protein with an additional 19 amino acids inserted in the C-half. The second cDNA sequence (NPIP2) contains a longer exon 1 transcript that uses an alternative splice donor site. This is predicted to

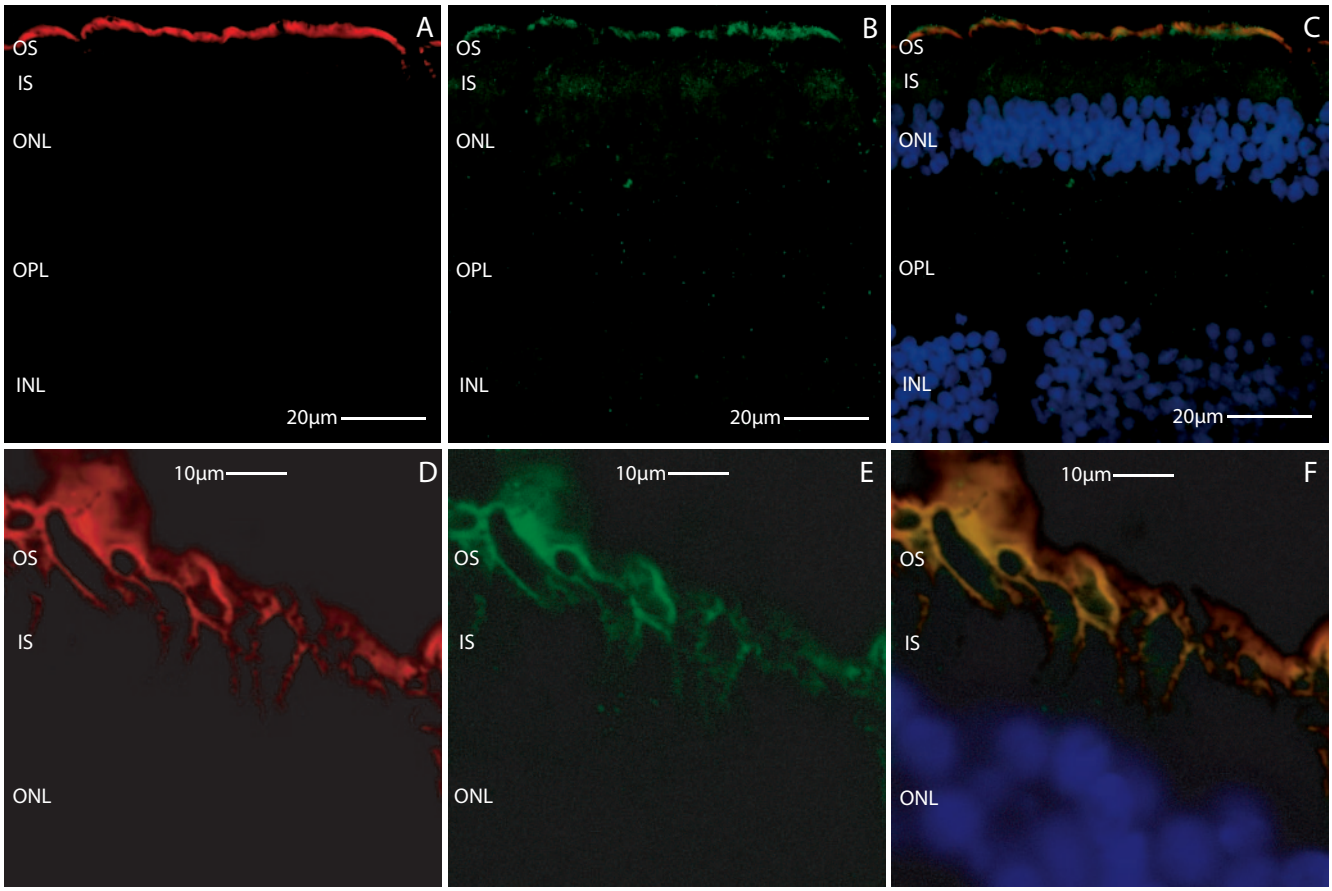

FIGURE 4. Confocal microscopy showing anti-NPIP and PNA staining in human fovea. At low magnification (*red*) PNA readily stains cone outer segments (**A**). Many outer segments also stain with (*green*) anti-NPIP (**B**, **C**). At high-magnification, the very close correspondence between PNA and anti-NPIP can be seen (**D**–**F**).

encode a very similar protein but without 123 amino acids of the N terminus. When GFP fusion constructs containing NPIP1 and NPIP2 were expressed by transient transfection, they localized to different SK-N-SH subcellular structures (see Supplementary Data). Whereas NPIP1 localized to the nuclear envelope region, NPIP2 appeared to be within the nucleus.

DISCUSSION

We analyzed differential gene expression in he macula compared with peripheral retina using microarrays and subsequently confirmed enrichment of 80% of genes, selected using strict criteria from the microarray data, by quantitative PCR. High expression levels were evident for several genes, and we localized two protein products to photoreceptor outer segments: NPIP and HDAC9. The results indicate that the primate-specific NPIP, enriched and highly expressed in the macula, is specifically localized to cone outer segments and contains a likely membrane localization signal in the N terminus of two or more isoforms.

From diagnostic analysis of the microarray data, *variance stabilization*[20] was chosen as the most appropriate method with which to perform calibration. Variance stabilization is a recent normalization algorithm that is designed to produce a constant signal-to-noise ratio over the entire dataset. This method allowed us to distinguish meaningful data from noise by using human macular mRNA. Furthermore, although many genes were found to be enriched in the macula according to the microarrays, only the few that fit strict data-mining criteria were studied further. Similarly, using a sample pooling approach together with an amplification plot method of efficiency calculation,[21] we were able to obtain reasonable estimates of macular gene expression relative to the opsins.

The gene products of *NPIP*, *GCN2*, *SRGAP3*, and *HDAC9* were previously uncharacterized in the retina. Our data provide evidence that these transcripts are macula-enriched and that *NPIP* and *GCN2* represent a significant proportion of the macular transcriptome. Only *SRGAP3* is as yet associated with a monogenic disease phenotype, in which abnormal development of neuronal structures leads to mental retardation.[25] However, *NPIP* (16p13-11), *GCN2* (15q15) and *SRGAP3* (3p25) are all located within possible regions of linkage suggested by whole-genome screens of age-related maculopathy.[28,29,30]

We localized full-length *HDAC9* to the nucleus of cultured cells, as would be expected by its HDAC activity and as previously reported.[22] However, it was also localized to filamentous structures. Of note, HDAC6 has been found to act as a molecular motor in the cytoskeleton.[31] In the human fovea, we found that HDAC9 localized to photoreceptors, especially the outer segments. Transcriptional repression (by histone deacetylation) may have a protective role in neuronal ageing and degeneration by preventing a stress response that leads to apoptosis of neuronal cells.[32] It is also possible that HDAC9 is involved in maintaining structural integrity in the photoreceptor via cytoskeletal elements and/or protein trafficking, perhaps via the ubiquitin-proteasome degradation system.[33] This

possibility may be especially important in the extremely cell dense macula.

NPIP is a member of a gene family originating from human chromosome 16 (LCR16a) that has been duplicated very recently and evolved rapidly.[27] It is an extreme example of positive selection, with up to 43% divergence of amino acids between primates, a hallmark of adaptive evolution. BLAST analysis of the reference sequence against dbEST or searching for motifs with PROSITE confirmed that NPIP is primate specific. Strikingly, among mammals it is only primate retinas that possess a macula. (Birds, such as hawks, have a very different retinal structure and can be bifoveate.) Apart from approximately 25% similarity with chicken caldesmon (NP_989489), and a portion of an archaeal coiled coil domain (NP_613407), there are no significant similarities of NPIP with any other known protein. Johnson et al.[27] described eight exons for NPIP, determined by genomic sequence analysis and reported a single putative transmembrane domain (from amino acid 54-72) surrounded by α-coil.

This is the first report to our knowledge of tissue localization of NPIP. It is of particular interest that NPIP is localized to cone photoreceptor outer segments in humans and that NPIP appears to be a significant part of the macular transcriptome. The longer novel isoform NPIP1 and the reference isoform AAD34394[27] localize to the nuclear envelope, whereas the shorter novel isoform NPIP2 localizes within the nucleus of cultured cells. This suggests that there is a membrane localization signal at the N terminus of the longer isoforms. It may be this same localization signal that directs NPIP to the outer segments of human cone photoreceptors although this, along with ultrastructural localization, remains to be seen.

Although the role of NPIP in cone photoreceptors remains unclear, it is of interest that other proteins thought to be associated with the nuclear pore also have a function in photoreceptors. For example, the *Drosophila* eyes closed gene (*Eyc*, an analogue of p47) is involved in both nuclear envelope and photoreceptor membrane reorganization.[34] There is also some evidence that RanBP2, a large protein that binds the nuclear pore–associated GTPase Ran, is highly expressed in cone photoreceptors of the vertebrate retina.[35] Indeed, RanBP2 was thought to be a chaperone for red/green cone opsin.

Autosomal recessive retinitis pigmentosa (arRP) has been linked to a chromosomal region that overlaps with NPIP (16p12.3-p12.1).[36] However, one of the two families showed physical signs frequently seen in patients with BBS (Bardet-Biedl syndrome). The other family reported night blindness from the second decade, which is characteristic of rod–cone dystrophy, although no retinal electrophysiology was published. NPIP is located within a region of suggested linkage (16p12) obtained from three separate genome-wide scans of age-related maculopathy[28–30] and an additional genome-wide scan for predisposition to Drusen formation.[37]

Characterizing macula enriched transcripts is an important stepping-stone in understanding the molecular basis for visual acuity in the retina. This approach also provides excellent candidates for diseases that affect the macula and fovea such as AMD. Work to define roles for *NPIP* and the other genes highlighted in this study is ongoing.

Acknowledgments

The authors thank the Eye Bank of British Columbia (Canada) and also Arthur Zelent's laboratory at the Institute of Cancer Research (UK) for support, advice, and encouragement.

References

1. Hendrickson A. Primate foveal development: a microcosm of current questions in neurobiology. *Invest Ophthalmol Visual Sci*. 1994;35:3129–3133.
2. Bernstein S, Borst D, Neuder M, Wong P. Characterization of a human fovea cDNA library and regional differential gene expression in the human retina. *Genomics.* 1996;32:301–308.
3. Sharon D, Blackshaw S, Cepko C, Dryja T. Profile of the genes expressed in the human peripheral retina, macula, and retinal pigment epithelium determined through serial analysis of gene expression (SAGE). *Proc Natl Acad Sci*. 2002;99:315–320.
4. O'Shea J. Age-related macular degeneration. *Postgrad Med J*. 1998; 74:203–207.
5. Evans W, Wormald R. Is the incidence of registrable age-related macular degeneration increasing? *Br J Ophthalmol*. 1996;80:9–14.
6. Heiba I, Elston R, Klein B, Klein R. Sibling correlations and segregation analysis of age-related maculopathy: the beaver dam eye study. *Genet Epidemiol*. 1994;11:51–67.
7. Meyers S, Greene T, Gutman F. A twin study of age-related macular degeneration. *Am J Ophthalmol*. 1995;120:757–766.
8. Klaver C, Wolfs R, Assink J, et al. Genetic risk of age-related maculopathy population-based familial aggregation study. *Arch Ophthalmol*. 1998;116:1646–1651.
9. Gottfredsdottir M, Sverrisson T, Musch D, Stefánsson E. Age related macular degeneration in monozygotic twins and their spouses in Iceland. *Acta Ophthalmol Scand*. 1999;77:422–425.
10. Edwards AO, Iii RR, Abel KJ, et al. Complement factor H polymorphism and age-related macular degeneration. *Science*. 2005;308: 421–424.
11. Haines JL, Hauser MA, Schmidt S, et al. Complement factor H variant increases the risk of age-related macular degeneration. *Science*. 2005;308:419–421.
12. Klein RJ, Zeiss C, Chew EY, et al. Complement factor H polymorphism in age-related macular degeneration. *Science*. 2005;308: 385–389.
13. Hageman G, Anderson D, Johnson L, et al. A common haplotype in the complement regulatory gene factor h (hf1/cfh) predisposes individuals to age-related macular degeneration. *Proc Natl Acad Sci USA*. 2005;102:7227–7232.
14. Gold B, Merriam JE, Zernant J, et al. Variation in factor B (BF) and complement component 2 (C2) genes is associated with age-related macular degeneration. *Nat Genet*. 2006;38:458–462.
15. Dewan A, Liu M, Hartman S, et al. HTRA1 promoter polymorphism in wet age-related macular degeneration. *Science*. 2006;314:989–992.
16. Yang Z, Camp NJ, Sun H, et al. A variant of the HTRA1 gene increases susceptibility to age-related macular degeneration. *Science*. 2006;314:992–993.
17. Kennan A, Aherne A, Palfi A, et al. Identification of an impdh1 mutation in autosomal dominant retinitis pigmentosa (rp10) revealed following comparative microarray analysis of transcripts derived from retinas of wild-type and rho(−/−) mice. *Hum Mol Genet*. 2002;11:547–557.
18. Freund C, Gregory-Evans C, Furukawa T, et al. Cone-rod dystrophy due to mutations in a novel photoreceptor-specific homeobox gene (CRX) essential for maintenance of the photoreceptor. *Cell*. 1997;91:543–553.
19. Livesey F, Furukawa T, Steffen M, et al. Microarray analysis of the transcriptional network controlled by the photoreceptor homeobox gene crx. *Curr Biol*. 2000;10:301–310.
20. Huber W, von Heydebreck A, Sultmann H, et al. Variance stabilization applied to microarray data calibration and to the quantification of differential expression. *Bioinformatics*. 2002;18:S96–S104.
21. Peirson S, Butler J, Foster R. Experimental validation of novel and conventional approaches to quantitative real-time pcr data analysis. *Nucleic Acids Research*. 2003;31:e73.
22. Petrie K, Guidez F, Howell L, et al. The histone deacetylase 9 gene encodes multiple protein isoforms. *J Biol Chem*. 2003;2:16059–16072.

23. Chen Y, Dougherty E, Bittner M. Ratio-based decisions and the quantitative analysis of cDNA microarray images. *J Biomed Opt*. 1997;2:364–374.
24. Harding H, Novoa I, Zhang Y, et al. Regulated translation initiation controls stress-induced gene expression in mammalian cells. *Mol Cell*. 2000;6:1099–1108.
25. Endris V, Wogatzky B, Leimer U, et al. The novel rho-gtpase activating gene megap/srgap3 has a putative role in severe mental retardation. *Proc Nat Acad Sci USA*. 2002;99:11754–11759.
26. Nagase T, Ishikawa K, Suyama M, et al. Prediction of the coding sequences of unidentified human genes. XI. The complete sequences of 100 new cDNA clones from brain which code for large proteins in vitro. *DNA Res*. 1998;5:277–286.
27. Johnson M, Viggiano L, Bailey J, et al. Positive selection of a gene family during the emergence of humans and African apes. *Nature*. 2001;413:514–519.
28. Schick J, Iyengar S, Klein B, et al. A whole-genome screen of a quantitative trait of age-related maculopathy in sibships from the Beaver Dam Eye Study. *Am J Hum Genet*. 2003;72:1412–1424.
29. Iyengar SK, Song D, Klein BEK, et al. Dissection of genomewide-scan data in extended families reveals a major locus and oligogenic susceptibility for age-related macular degeneration. *Am J Hum Genet*. 2004;74:20–39.
30. Schmidt S, Scott W, Postel E, et al. Ordered subset linkage analysis supports a susceptibility locus for age-related macular degeneration on chromosome 16p12. *BMC Genet*. 2004;5:18.
31. Kopito RR. The missing linker: an unexpected role for a histone deacetylase. *Mol Cell*. 2003;12:1349–1351.
32. Salminen A, Tapiola T, Korhonen P, Suuronen T. Neuronal apoptosis induced by histone deacetylase inhibitors. *Brain Res Mol Brain Res*. 1998;61:203–206.
33. Lipford JR, Deshaies RJ. Diverse roles for ubiquitin-dependent proteolysis in transcriptional activation. *Nat Cell Biol*. 2003;5:845–850.
34. Sang TK, Ready DF. Eyes closed, a Drosophila p47 homolog, is essential for photoreceptor morphogenesis. *Development*. 2002; 129:143–154.
35. Ferreira P, Nakayama T, Pak W, Travis G. Cyclophilin-related protein RanBP2 acts as chaperone for red/green opsin. *Nature*. 1996; 383:637–640.
36. Finckh U, Xu S, Kumaramanickavel G, et al. Homozygosity mapping of autosomal recessive retinitis pigmentosa locus (RP22) on chromosome 16p12.1-p12.3. *Genomics*. 1998;48:341–345.
37. Jun G, Klein BEK, Klein R, et al. Genome-wide analyses demonstrate novel loci that predispose to drusen formation. *Invest Ophthalmol Vis Sci*. 2005;46:3081–3088.